Theor Chem Acc (2011) 130:901–907
DOI 10.1007/s00214-011-0971-3

REGULAR ARTICLE

The [2 + 2 + 2] mechanisms of trimerization of three ethynes and monosilaethylenes

Homologous concerted mechanism and polarized one-step mechanism

Shogo Sakai · Keitaro Taketa

Received: 21 December 2010 / Accepted: 31 May 2011 / Published online: 23 June 2011

Abstract The mechanisms of [2 + 2 + 2] reactions of three ethynes and monosilaethylenes to form benzene and 1,3,5-trisilacyclohexane were studied by ab initio MO methods. The reaction mechanisms were analyzed by configuration interaction/localized molecular orbital/CASSCF calculations. Although the [2 + 2 + 2] reaction of ethyne is typically “homologous” concerted, that of monosilaethylene is polarized (ionic-cyclic) one-step reaction. In addition, the aromaticity along the intrinsic reaction coordinate pathway was studied using the index of deviation from aromaticity. Although the transition state of trimerization of ethyne does not have an aromatic nature for the σ- and π-bonds formation system, the crossing point of the σ-bond formation and π-bond breaking shows an aromatic nature.

Keywords [2 + 2 + 2] peri cyclic reaction mechanism · Aromaticity · Ab initio MO

1 Introduction

The trimerization of ethyne to yield benzene is a prototypical [2 + 2 + 2] cyclic addition and is classified as a thermally allowed reaction on the basis of Woodward–Hoffmann rules [1]. Despite being extremely exothermic, the reaction occurs only to a small extent at temperatures in excess of 400 °C. Since the reaction’s discovery in 1866 by Berthelot and co-workers [2, 3], its mechanisms attracted much theoretical and experimental interest [4–17]. Recently, Santos and co-workers [17] evaluated the energy barrier of trimerization of ethyne as 53.1 kcal/mol by the CCSD(T)/6-311G(d,p) level. The trimerization of ethyne to form benzene is also interesting because of its “aromaticity” via the concerted pathway that passes through the transition state with the (4n + 2) electrons resonance state. However, there is some debate over the σ and π contributions to the possible aromaticity at the transition state. Jiao and Schleyer [9] concluded from the nucleus-independent chemical shifts (NICS) values that both σ and π electrons made significant contributions to the diatropic ring current at the transition state. Mora and Cossio [10] concluded from a study of the height profile of NICS values that there is no π aromaticity in the transition state. By analysis of current density maps, Havenith et al. [14] showed an induced circulation of σ electrons but no π contribution at the transition state. Santos and co-workers [15] also studied the aromaticity along the reaction pathway by the electron localization function (ELF) and pointed out a low σ-electron delocalization at the transition state. Thus, the evaluation of aromaticity at the transition state depends on the measurement indices of aromaticity. In previous papers [18–20], we proposed a new index of aromaticity, the index of deviation from aromaticity (IDA), on the basis of configuration interaction/localized molecular orbital/CASSCF (CiLC) analysis. The IDA indicates [21, 22] an excellent relationship between aromaticity and stabilization energy for many polycyclic and/or nonplanar compounds, whereas an index based on magnetic diatropic ring current, for example, the NICS values sometimes incorrectly estimate [21, 23] some species, e.g., polycyclic and nonplanar compounds. Therefore, it is important to evaluate the

---

Dedicated to Professor Akira Imamura on the occasion of his 77th birthday and published as part of the Imamura Festschrift Issue.

S. Sakai (✉) · K. Taketa
Department of Chemistry, Faculty of Engineering
Gifu University, Yanagido, Gifu 501-1193, Japan
e-mail: sakai@gifu-u.ac.jp

reaction mechanisms and aromaticity along the reaction pathways.

The [2 + 2 + 2] cyclic reaction composed of polarized π orbitals is also interesting in comparison with the mechanism of homologous π orbitals as ethyne. Therefore, we studied the [2 + 2 + 2] cyclic reaction of Si–C σ–bond formation from π bonds. Although monosilaethylene has the structure similar to ethyne, the geometry is different. The geometry of ethyne is linear, but that of monosilaethylene is not linear from the calculation by the B3LYP method. Schaefer and co-workers [24] showed trans-bent structure for monosilaethylene by CI calculation level. Thus, monosilaethylene does not have π bond composed from only two p orbitals. On the other hand, monosilaethylene has the π bond similar to that of ethyne. Therefore, to study the difference in the [2 + 2 + 2] mechanisms between homologous π bonds and little polarized π bonds, the trimerization of monosilaethylene is treated here.

In this paper, we report the reaction mechanisms and aromaticity along the reaction pathways of the trimerization of ethyne and monosilaethylene by using CiLC analysis and IDA calculations.

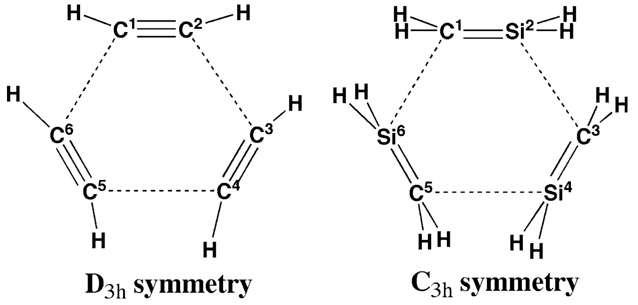

2 Theoretical treatments

The equilibrium- and transition-state geometries for the reactions treated here were determined using a CASSCF MO method [25] and/or the B3LYP density functional method [26, 27] with analytically calculated energy gradients. For the reaction of three ethynes, two types of active spaces for the CASSCF calculation were treated, because the two groups of the orbitals are orthogonal to each other. One is six active orbitals with six electrons relating to direct formation of σ bonds from π orbitals (defined as side π) of ethyne for a D_{3h} symmetry structure. The other is six active orbitals with six electrons relating to π-bond formation of benzene from π orbitals of ethyne. The first treatment of CASSCF calculation was used for the determination of geometry, the estimation of energy, and the CiLC analysis. The second treatment was used for the CiLC analysis. For the CASSCF calculation of trimerization of monosilaethylene, the same active spaces were chosen as for the first treatment of ethyne. All configurations in active spaces were generated, and a vibrational analysis was performed at each stationary point to confirm its identity as either an energy minimum or a transition state structure. Additional calculations were made to obtain improved energy comparison calculations for CASSCF-optimized structures with electron correlation incorporated through the multiconfigurational second-order perturbation theories (MRMP2) [28] with the 6-31G(d) and 6-311+G(d,p) basis sets [29–31]. The intrinsic reaction coordinate (IRC) [32, 33] was followed from the transition state toward both reactants and products.

To interpret the mechanisms of the reactions, a CiLC analysis was performed following a method described elsewhere [34–38]. First of all, the CASSCF calculation is made for the active orbitals. After carrying out the CASSCF procedure, the CASSCF-optimized orbitals are localized by the Boys localization procedure [39, 40]. The calculated localized orbitals are very atomic in nature. By using the localized MOs as a basis, a full CI with the determinant level is used to generate electronic structures and their relative weights in the atomic orbital-like wave functions. Then, we obtain many coefficients, which correspond to each configuration. But it is not easy to find the relation between the obtained coefficients (or weights: the square of coefficients) and the chemical bonds and/or the chemical reactions. So we think that the obtained configurations are constituted from the configurations represented each bond state and the reference state (alternative spin for neighboring orbitals). Then, we introduce one hypothesis: the configurations of one bond are presented roughly as one singlet-coupling (covalent) term and two polarization (ionic) terms. The singlet-coupling term has alternative spin in the pair orbitals of the bond, and the pair orbitals have same spin with the neighboring orbitals of each side. All orbitals except the pair orbitals of the bond have alternative spin for neighboring orbitals. The polarization (ionic) terms mean one electron movement in the pair orbitals of the bond. The other configurations are considered as the higher order excited states or the mix states for the configurations of the bonds. It is also considered that the weight of the reference configuration, which has usually the largest coefficient, does not affect the variation in geometry. Here, we think the region of the neighboring orbitals with same spin is similar to the concept of the phase of anti-bonding orbital. In figure, the circle with solid line indicates an atomic-like orbital obtained by the localization process in the CiLC calculations and the circle with dotted line means a bond.

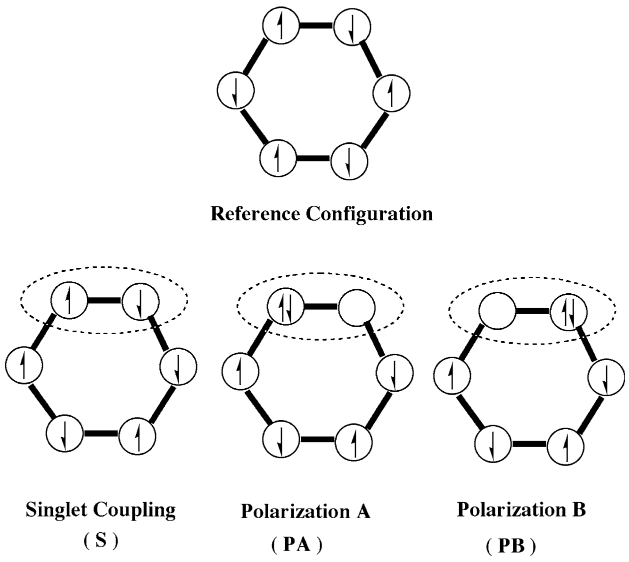

The representation with three terms (one singlet-coupling (covalent) and two polarization (ionic) terms) for a bond has successfully explained [35–38, 41–46] bond formation and breaking along a chemical reaction path.

The criterion of aromaticity was defined [18–20] according to the following conditions on the basis of the CiLC calculations: (a) each weight of the singlet-coupling (covalent) and polarization (ionic) terms is equal for all bonds and (b) the difference between the weights of the singlet-coupling and polarization terms for each bond is small. The first criterion is general and more expanded representation of "the bond length equalization [47]", which is one of many proposed aromatic criterions. The second means much resonance stabilization energy for each bond. Namely the aromaticity defined here demands the same electronic state for all bonds and the much resonance energy for each bond. From the two criteria of aromaticity, the IDA for an n-cyclic ring can be defined by equations (1–4):

$$IDA = D_s + D_p + G_{sp} \tag{1}$$

$$D_s = \frac{\left(\sum_{i=1}^{n} \left|\frac{S_i - S_{av}}{S_{av}}\right|\right)}{n} \tag{2}$$

$$D_p = \frac{\left(\sum_{i=1}^{n} \frac{|PA_i - P_{av}| + |PB_i - P_{av}|}{2P_{\mathrm{av}}}\right)}{n} \tag{3}$$

$$G_{sp} = \frac{\left(\sum_{i=1}^{n} \frac{|S_i - PA_i| + |S_i - PB_i|}{2S_i}\right)}{n}, \tag{4}$$

where S_{i} is the weight of the singlet-coupling term for the ith bond, S_{av} is the average of the weights of the singlet-coupling terms for all bonds, PA_i and PB_i are the weights of the polarization terms for the ith bond, P_{av} is the average of the weights of the polarization terms for all bonds, and n is the number of bonds in the ring. Here, D_s and D_p are the ratios of deviation from the average weights of the singlet-coupling and polarization terms, respectively, and they correspond to the requirement of criterion (a). The term G_{sp} denotes the average ratio of the difference between the weights of the singlet-coupling and polarization terms on the basis of the average singlet coupling.

The calculations of the CiLC analysis and MRMP2 method were made using the GAMESS program package [48, 49], and the other calculations were made using the Gaussian03 program package [50].

3 Results and discussion

3.1 Trimerization of ethyne

The transition state geometries of [2 + 2 + 2] type trimerization of ethyne were obtained by the B3LYP/6-31G(d) method, the CASSCF(6,6)/6-31G(d), and CASSCF(6,6)/6-311+G(d,p) calculation levels (Fig. 1).

The C–C bond distances obtained by the B3LYP method are slightly longer than those obtained by the CASSCF levels. The transition state with one negative eigenvalue for the force-constant matrix has D_{3h} symmetry at the methods used here, and the activation energy barriers are 42.1 kcal/mol, 68.6 kcal/mol, and 73.4 kcal/mol by the B3LYP/6-31G(d), CASSCF/6-31G(d), and CASSCF/6-311+G(d,p) methods, respectively. Although the activation energy barriers obtained by the CASSCF calculations are larger than those obtained by the B3LYP and CCSD(T) methods,

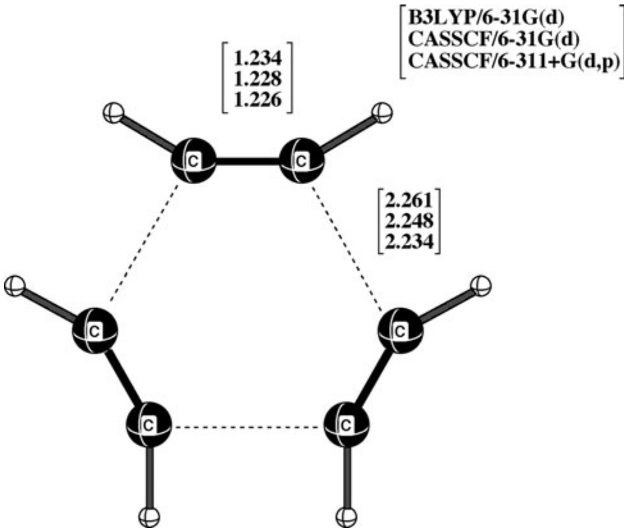

Fig. 1 Geometric parameters of the transition state of trimerization of ethyne. Bond lengths are in Å

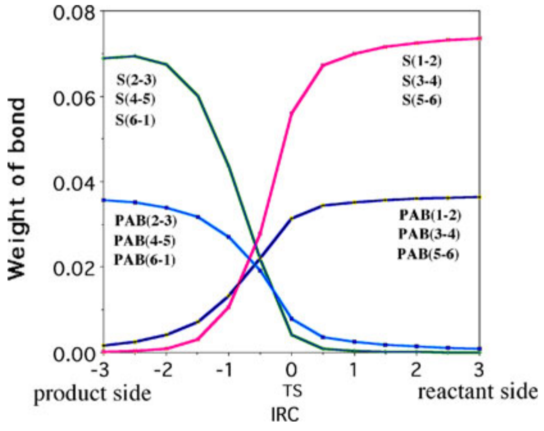

Fig. 2 Weights of σ-side π bonds of CiLC calculation along the IRC pathway of trimerization of ethyne. The units at the abscissa are bohr amu$^{1/2}$

the energies including dynamical correlation obtained by the MRMP2/6-31G(d) and MRMP2/6-311+G(d,p) methods are 42.1 kcal/mol and 41.4 kcal/mol, respectively.

To study the electronic states of each bond along the reaction path, the weights of the singlet-coupling and polarization terms of each σ-bond formation from the side π orbitals along the IRC pathway (obtained by the B3LYP level) are shown in Fig. 2; S(x–y) and PAB(x–y) indicate the weights of the singlet-coupling and polarization (PA and PB) terms between x and y atoms (orbitals).

The crossing point between the side π-bond breaking (C^1–C^2, C^3–C^4, and C^5–C^6 bonds) and the σ-bond formation (C^2–C^3, C^4–C^5, and C^6–C^1 bonds) is located slightly toward the product side (about -0.5 bohr amu$^{1/2}$ from the transition state). The variation in these bonds along the IRC pathway is a typical "homologous concerted mechanism". From the variations in these terms, the process of the side π breaking and new σ-bond formation occurs in the area from 1 bohr amu$^{1/2}$ to -2 bohr amu$^{1/2}$ along the IRC pathway.

The weights of the singlet-coupling and polarization terms of each π bond relating to π orbitals of benzene along the IRC pathway are shown in Fig. 3.

The weights of the singlet-coupling and polarization terms of the old π bonds (C^1–C^2, C^3–C^4, and C^5–C^6) and the new π bonds (C^2–C^3, C^4–C^5, and C^6–C^1) approach each other in the area of -8 bohr amu$^{1/2}$ along the IRC pathway. The variable decrease in the old π bonds is an interesting point. Although the polarization terms of the old π bonds decrease smoothly, the weights of the singlet-coupling terms of the old π bonds is a maximum at approximately -3 bohr amu$^{1/2}$ along the IRC pathway. This means the reorganization from the π orbitals of ethyne to the π orbitals of benzene occurs after the exchange between the side π orbitals and the new σ orbitals through the transition state.

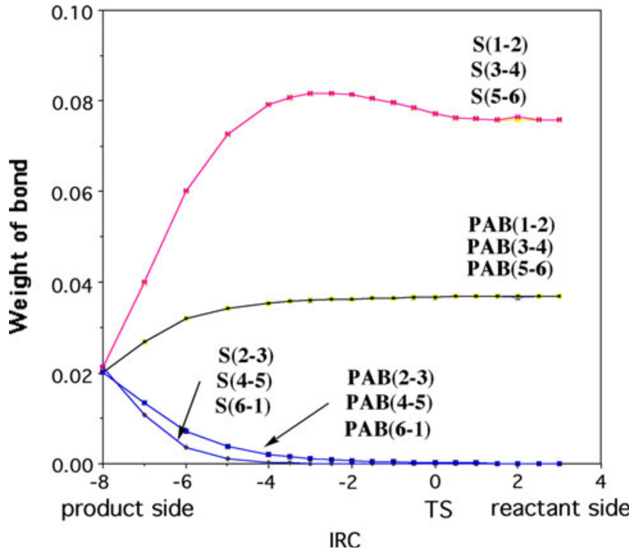

Fig. 3 Weights of π bonds of CiLC calculation along the IRC pathway of trimerization of ethyne. The units at the abscissa are bohr amu$^{1/2}$

The IDA values for σ- (side π) and π-bond formations along the IRC pathways are shown in Figs. 4 and 5.

The minimum value of IDA for σ-bond formation is approximately -0.5 bohr amu$^{1/2}$ along the IRC pathway and corresponds to the crossing point between old π-bond breaking and new σ-bond formation (Fig. 2). The IDA value at the transition state is 2.159 that indicates non-aromaticity [51]. The nature of aromaticity at the transition state corresponds to the results of the current density map analysis [14]. The IDA value at the crossing point (-0.5 bohr amu$^{1/2}$) is 0.356 that indicates aromatic nature. The

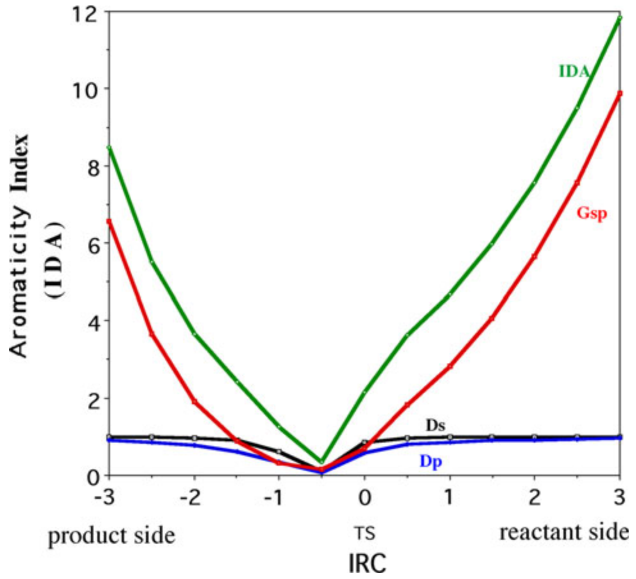

Fig. 4 IDA values of σ-side π bonds along the IRC pathway of trimerization of ethyne. The units at the abscissa are bohr amu$^{1/2}$

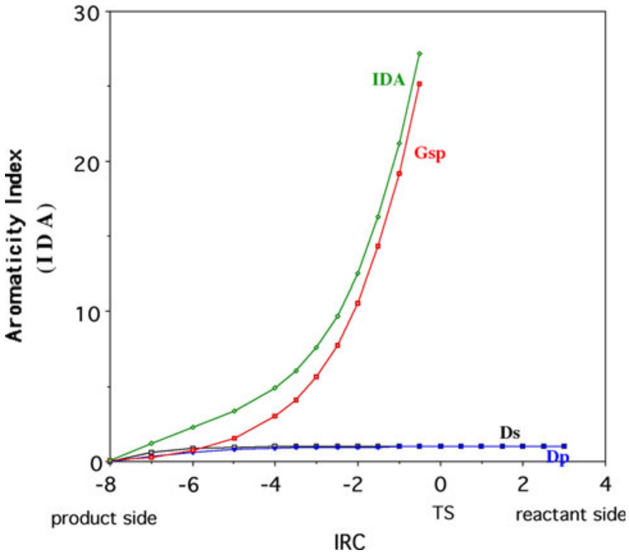

Fig. 5 IDA values of π bonds along the IRC pathway of trimerization of ethyne. The units at the abscissa are bohr amu$^{1/2}$

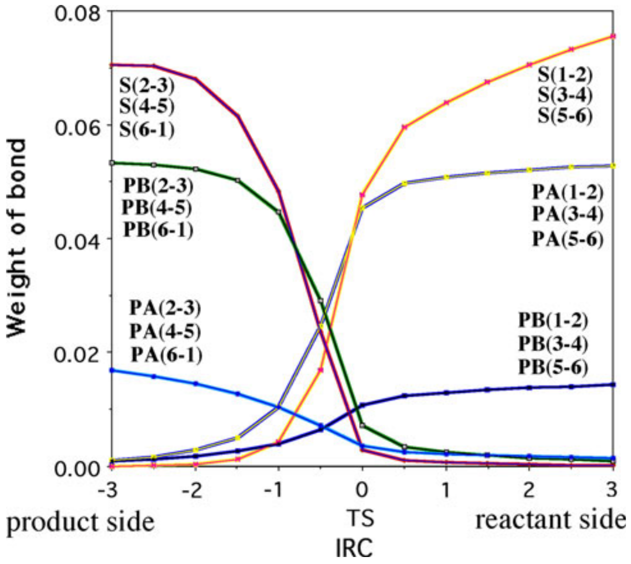

Fig. 6 Weights of bonds of CiLC calculation along the IRC pathway of trimerization of monosilaethylene. The units at the abscissa are bohr amu$^{1/2}$

aromatic nature at the crossing point indicates a "homologous concerted mechanism", and it is similar to the Diels–Alder reaction. The IDA value [22] at the transition state of the Diels–Alder reaction of butadiene and ethylene is 0.268, where the crossing point between the weights of the breaking and formation bonds of the Diels–Alder reaction corresponds [37] to the transition state. For the aromaticity of the π-bond formation, the IDA values decrease from the reactant side to the product side (Fig. 5) and approach almost the IDA value (0.047) [18] of benzene at -8 bohr amu$^{1/2}$ of the IRC pathway. The IDA value at the transition state is extremely large and suggests a non-aromatic nature of π bonds.

3.2 Trimerization of monosilaethylene

The transition state for trimerization of monosilaethylenes was calculated by the CASSCF/6-31G(d) level. The distances of the intramolecular and intermolecular C–Si of the transition state are 1.739Å and 2.896Å lengths, respectively. Although the transition state was also tried to obtain by the B3LYP method, it could not be found. Therefore, we used the transition state geometry and the IRC pathway obtained by the CASSCF method for the analysis of the mechanism. The transition-state structure has C_{3h} symmetry. The activation energy barrier is 6.3 kcal/mol by the CASSCF(6,6)/6-31G(d) level and disappears by the MRMP2 calculation levels with 6-31G(d) and 6-311+G(d,p) basis sets. The energy barrier is much lower than that of the trimerization reaction of ethyne or ethylene (energy barrier 42.1 kcal/mol for ethyne and 49.7 kcal/mol for ethylene [52] at the B3LYP/6-31G* level). The weights of singlet and polarization terms of each bond along the IRC pathway for trimerization of monosilaethylene are shown in Fig. 6.

In the figure, PA(x–y) means the electron pairs polarized to an x atom (orbital), and PB(x–y) means the electron pairs polarized to a y atom (orbital). The crossing points of the weights of the terms of the breaking and the formation of bonds are located in the region -0.5 bohr amu$^{1/2}$ of the products side, and the locations of the crossing points are similar to those of ethyne (Fig. 2). However, the π electrons of the Si–C bond are extremely localized on the C atom. At the crossing points, the weights of the polarization terms localized on the C atom are larger than those of the singlet-coupling terms, and those localized on the Si atom are extremely small.

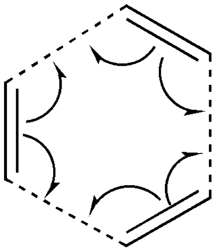

homologous Concerted Mechanism

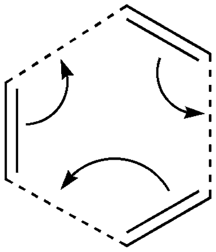

Polarized one-step Mechanism

The reaction occurs through the "polarization" (ionic-cyclic) mechanism. To compare the "homologous concerted" and "polarization one-step" mechanisms, the diradical and polarized state of ethylene and monosilaethylene were

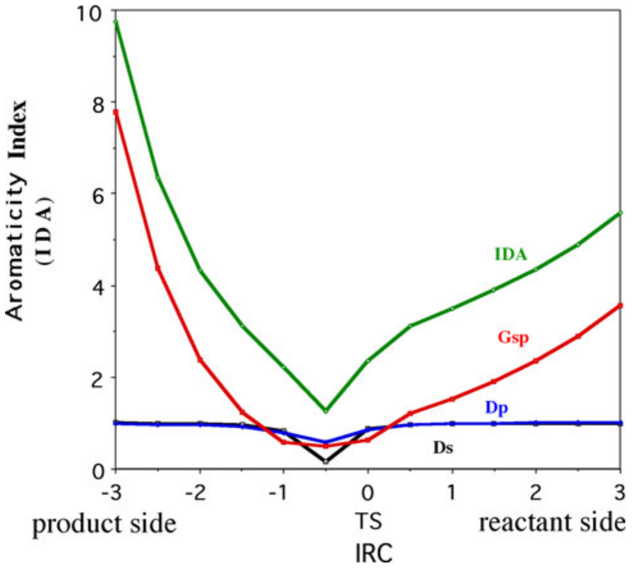

Fig. 7 IDA values of π bonds along the IRC pathway of trimerization of monosilaethylene. The units at the abscissa are bohr amu$^{1/2}$

calculated by the CASSCF level, assuming twisted structures with an angle of 90° with the C–C or C–Si bond axis. Although the diradical state of ethylene is approximately 78 kcal/mol lower than the polarization state, the diradical state of monosilaethylene is approximately 7 kcal/mol higher than the polarization state. Thus, the energy comparison of the diradical and polarization states corresponds to the polarization one-step mechanism of the trimerization of monosilaethylene.

To study the aromaticity along the IRC pathway of trimerization of monosilaethylene, the IDA values are shown in Fig. 7.

The minimum IDA value is located in the region around -0.5 bohr amu$^{1/2}$ along the IRC pathway and corresponds to the crossing point between the breaking and the formation of bonds, as shown above. The IDA value at -0.5 bohr amu$^{1/2}$ along the IRC pathways is 1.258, and at the transition state is 2.360. The IDA values of both points are larger than those of the trimerization of ethyne and indicate nonaromatic nature. The IDA value (1.258) at the crossing point is slightly smaller than the IDA value (1.345) [21] at the transition state of the "symmetry forbidden" cyclic reaction of 1,3,5-hexatriene.

4 Conclusions

The trimerization mechanisms of three ethynes and monosilaethylenes were studied by the CASSCF MO and B3LYP methods. The mechanisms and the aromaticity were analyzed by the CiLC method and IDA calculations.

For the trimerization of ethyne, the reaction is a typical homologous concerted mechanism. The crossing points between the side π-orbital breaking and the σ-bond formation occur after the transition state. Although the large IDA value indicates the transition state is nonaromatic, the crossing point shows aromatic nature. On the other hand, the π-bond formation proceeds monotonically, and the region around the transition state has a large IDA value.

For the reaction of monosilaethylene, the reaction mechanism is not homologous concerted, but polarized one-step. The mechanism corresponds to the IDA values at the transition state and/or the crossing point between bond breaking and formation. Specifically, the IDA values at both points of the transition state and the crossing point are large and indicate nonaromatic nature. The difference between the mechanisms of trimerization of ethyne and monosilaethylene probably relates closely to the activation energy barriers.

Acknowledgment The present research is supported by a Grant-in-Aid for Scientific Research from the Ministry of Education Science and Culture of Japan. The computer time was made available by the Computer Center of the Institute for Molecular Science.

References

1. Woodward RB, Hoffmann R (1970) The conservation of orbital symmetry. Verlage Chemie, Weinheim
2. Berthelot M (1866) C R Acad Sci 62:905. doi:10.1002/jlac.18661390303 (see: http://www.biodiversitylibrary.org/item/23761#page/913/mode/1up)
3. Berthelot M (1866) Ueber die Einwirkung der Hitze auf einige Kohlenwasserstoffe. Justus Liebigs Annalen der Chemie 139: 272–282. (see: http://www.archive.org/details/annalenderchemi11liebgoog)
4. Zimmerman HE (1971) Acc Chem Res 4:272
5. Houk KN, Gandour R, Strozier R, Rondan N, Paquette L (1979) J Am Chem Soc 101:6797
6. Bach RD, Wolber GJ, Schleyer HB (1985) J Am Chem Soc 107:2837
7. Ioffe A, Shaik S (1992) J Chem Soc Perkin Trans 2:2101
8. Wagenseller PE, Birney DM, Roy D (1995) J Org Chem 60:2853
9. Jiao H, Schleyer PvR (1998) J Phys Org Chem 11:655
10. Morao I, Cossio F (1999) J Org Chem 64:1868
11. Sawicka D, Wilsey S, Houk KN (1999) J Am Chem Soc 121:864
12. Sawicka D, Li Y, Houk KN (1999) J Chem Soc Perkin Trans 2:2349
13. Cioslowski J, Liu G, Moncrieff D (2000) Chem Phys Lett 316:536
14. Havenith R, Fowler P, Jenneskens L, Steiner E (2003) J Phys Chem A 107:1867
15. Santos JC, Polo V, Andres J (2005) Chem Phys Lett 406:393
16. Eichberg MJ, Houk KN, Lehmann J, Leonard PW, Marker A, Norton JE, Sawicka D, Vollhardt KPC, Whitener GD, Wolff S (2007) Angew Chem Int Ed 46:6894
17. Donoso-Tauda O, Aizman A, Escobar CA, Santos JC (2009) Chem Phys Lett 469:219
18. Sakai S (2002) J Phys Chem A 106:10370
19. Sakai S (2002) J Phys Chem A 106:11526
20. Sakai S (2003) J Phys Chem A 107:9422
21. Sakai S (2005) J Mol Struc (THEOCHEM) 715:101
22. Sakai S (2006) J Phys Chem A 110:6339

23. Fias S, Damme SV, Bultinck P (2008) J Comput Chem 29:358
24. Hoffmann MR, Yoshioka Y, Schaefer HF III (1983) J Am Chem Soc 105:1084
25. Roos B, (1987) In Advances in Chemical Physics; KP Lawley Ed; Wiley: New York, vol. 69, Part II, p 399
26. Becke AD (1988) Phys Rev A 38:3098
27. Lee C, Yang W, Parr RG (1988) Phys Rev B 37:785
28. Nakano H (1993) J Chem Phys 99:7983
29. Hariharan PC, Pople JA (1973) Theo Chim Acta 28:213
30. Gordon MS (1980) Chem Phys Lett 76:163
31. Krishnan R, Binkley JS, Seeger R, Pople JA (1980) J Chem Phys 72:650
32. Fukui K (1970) J Phys Chem 74:4161
33. Ishida K, Morokuma K, Komornicki A (1977) J Chem Phys 66:2153
34. Cundari T, Gordon M (1991) J Am Chem Soc 113:5231
35. Sakai S (1998) Chem Phys Lett 287:263
36. Sakai S, Takane S (1999) J Phys Chem A 103:2878
37. Sakai S (2000) J Phys Chem A 104:922
38. Sakai S (2002) Int J Quantum Chem 90:549
39. Boys SF (1960) Rev Mod Phys 32:296
40. Foster JM, Boys SF (1960) Rev Mod Phys 32:300
41. Lee PS, Sakai S, Horstermann P, Roth WR, Kallel EA, Houk KN (2003) J Am Chem Soc 125:5839
42. Sakai S, Nguyen MT (2004) J Phys Chem A 108:9169
43. Wakayama H, Sakai S (2007) J Phys Chem A 111:13575
44. Sakai S, Hikida T (2008) J Phys Chem A 112:10985
45. Yamada T, Udagawa T, Sakai S (2010) Phys Chem Chem Phys 12:3799
46. Sakai S, Yamada T (2008) Phys Chem Chem Phys 10:3861
47. Minkin VJ, Glukhovtsev MN, Simkin BY (1994) Aromaticity and antiaromaticity: electronic and structural aspects. Wiley, New York
48. Schmidt MW, Buldridge KK, Boatz JA, Elbert ST, Gordon MS, Jensen JH, Koseki S, Matsunaga N, Nguyen KA, Su S, Windus TL, Dupuis M, Montgomerry JA (1993) J Comput Chem 14:1347
49. Gordon MS, Schmidt MW (2005) Theory and applications of computational chemistry; the first forty years. In: Dykstra CE, Frenking G, Kim KS, Scuseria GE (eds) Elsevier, Amsterdam, pp 1167–1189
50. Frisch KJ, Trucks GW, Schlegel HB, Scuseria GE, Robb MA, Cheseman JR, Montgomery JA, Vreven Jr T, Kudin KN, Burant JC, Millam JM, Iyengar SS, Tomasi J, Barone V, Mennucci B, Cossi M, Scalmani G, Rega N, Petersson GA, Nakatsuji H, Hada M, Ehara M, Toyota K, Fukuda R, Hasegawa J, Ishida M, Nakajima T, Honda Y, Kitao O, Nakai H, Klene M, Li X, Knox E, Hratchian HP, Cross JB, Adamo C, Jaramillo J, Gomperts R, Stratmann RE, Yazyev O, Austin AJ, Cammi R, Pomelli C, Ochterski JW, Ayala PY, Morokuma K, Voth GA, Salvador P, Dannenberg JJ, Zakrzewski VG, Dapprich S, Daniels AD, Strain MC, Farkas O, Malick DK, Rabuck D, Raghavachari K, Foresman JB, Ortiz JV, Cui Q, Baboul AG, Clifford S, Cioslowski J, Stefanov BB, Liu G, Liashenko A, Piskorz P, Komaromi I, Martin RL, Fox DJ, Keith T, Al-Laham MA, Peng CY, Nanayakkara A, Challacombe M, Gill PMW, Johnson B (2003) Chen W, Wong MW, Gonzalez C, Pople JA, Gaussian 03; Gaussian, Inc.: Pittsburgh, PA
51. IDA value of benzene is 0.047 and that of cyclobutadiene with rectangular type is 2.037
52. Sawicka D, Li Y, Houk KN (1999) J Chem Soc Perkin Trans 2:2349